CVEL

THE CLEMSON UNIVERSITY VEHICULAR ELECTRONICS LABORATORY

TECHNICAL REPORT: CVEL-09-09

TIRE PRESSURE MONITORING SYSTEM (TPMS) EM PROPAGATION MODELING PROGRESS PART1: ANTENNA DESIGN

Hua Zeng and Todd Hubing

Clemson University

October 5, 2009

EXECUTIVE SUMMARY

This report investigates various antenna designs used by tire pressure monitoring systems (TPMS). Due to the small size requirements for TPMS modules that are mounted in tires, their antennas are typically much smaller than a wavelength at the frequency of operation. Different types of antennas made from a PCB trace or a separate metal piece are investigated, including loop antennas, whip antennas, and dipole antennas. The metal rim of the wheel also plays an important role in the antenna performance whether or not it is directly connected to the PCB. The impedance, radiation efficiency, and near fields of various antennas are determined, based on simulation results obtained using FEKO, a full-wave moment method code. The results show that electrically connecting the ground plane of the PCB to the metal rim can improve the radiation efficiency for both loop and whip antennas. A whip antenna made from a raised metal piece exhibits the best performance among the antennas investigated here in terms of radiation efficiency. However, further research is necessary to consider the larger near magnetic field of the loop antenna and the whole vehicle body effects.

I. INTRODUCTION

Automatic tire pressure monitoring has been required on all new vehicles sold in the U.S. since September 2007. Most of the tire pressure monitoring systems (TPMS) in vehicles today employ battery powered sensors in each of the tires that communicate wirelessly with a central unit located behind the dashboard. The batteries in these sensors cannot be replaced, so it is necessary to replace the entire sensor module, when the battery is too weak to provide a reliable signal. A number of functional issues have been documented with these systems, including false low-pressure warnings that occur when the TPMS signal is lost or interfered with. A significant technical challenge associated with TPMS systems is to ensure adequate sensor transmission/reception in the vehicle while using the limited sensor power efficiently.

V. Kukshya [1] introduced a system simulator to characterize the performance of tire pressure monitoring systems in various operational scenarios. K. Tanoshita [2] simulated the electric field characteristics of the AIRwatch system in Japan. H.J. Song [3] and M. Brzeska [4] presented RF models to model the signal strength range of TPMS. However, these results only illustrate the signal propagation between the transmitting module and receiver module and need to be verified by actual tests. In addition, other signal paths, such as the power transfer from an RFIC transmitter to its transmitting antenna have a significant impact on the total power budget and need to be addressed. Therefore, it is necessary to investigate the system noise margin systematically so that a TPMS designer can gain insight as to how to design tire pressure monitoring modules with greater power efficiency and reliability.

The goal of this project is to better understand the factors that affect the communication with TPMS sensors mounted inside a tire. The scope of the work is divided into three parts. The first part, which will be addressed in this report, is to investigate the antenna design, one of the most important issues faced by a TPMS system designer. The second part is to identify transmission parameters from a rotating tire and the vehicle body's effect on tire sensor transmission and propagation; and to relate these effects to receiver antenna packaging requirements. The third part is to determine a power budget based on an analysis of the total path loss and propose an optimized design. In addition, an improved test method will be developed that can be used to evaluate TPMS systems.

II. ANTENNA DESIGN AND SIMULATION

The physical size of a TPMS sensor module is restricted and is generally much smaller than the wavelength of interest. Therefore, the antennas in a TPMS sensor must be electrically small. The TPMS antennas used in the North American market generally operate at 315 MHz ($l \sim 1$ meter). They are usually not structurally self-resonant at this frequency and have a low radiation resistance and a large reactance. In order to save the power, the antennas utilize a matching network to cancel the reactance and transform the low radiation resistance to a larger input resistance.

Although the matching network can help reduce the mismatch loss, any loss in the antenna structure itself, or in the matching network can reduce the efficiency greatly due to the low radiation

resistance of the antenna. Since the total power transmitted from the TPMS module will be significantly limited by the antenna radiation efficiency, an antenna with high radiation efficiency is preferred. In this report, the radiation efficiency of three antenna structures: a small loop, a whip, and a dipole antenna are evaluated. In order to determine the impact of the wheel rim on a TPMS antenna's performance, three cases are investigated: the antenna without a rim, the antenna in electrical contact with a metal rim, and the antenna near, but not connected to, a metal rim.

A. Design Requirements

The RF circuitry is to be implemented on a 66 mm x 24 mm x 2mm printed circuit board. The bottom side is a ground plane. The antenna can be designed using a trace on the PCB or a separate raised piece of metal.

B. Antenna made from a PCB Trace

1) Case 1. Antenna structure without rim

Fig. 1 shows the geometry of small loop antenna, whip antenna, and dipole antenna from left to right respectively. The loop antenna could be fed single-ended or differentially. A single-ended antenna is employed in this research. The far end of the loop is grounded. The total loop length is 50 mm, the width 24 mm and the trace width is 2 mm. The ground plane does not extend into the region where the antenna structure is implemented while keeping the rest of the PCB area large enough to hold the other required circuitry. The whip antenna is single-ended and the far open end is kept away from the ground plane. The antenna arm is 50 mm long plus a 24 mm bent part. The bent arm makes the whip antenna more area efficient. The dipole antenna is a differentially driven structure with two bent arms. The dipole antenna is located along the edge of the board and kept away from the ground plane. A balun is usually required for this kind of antenna in order to interface with a single-ended amplifier output.

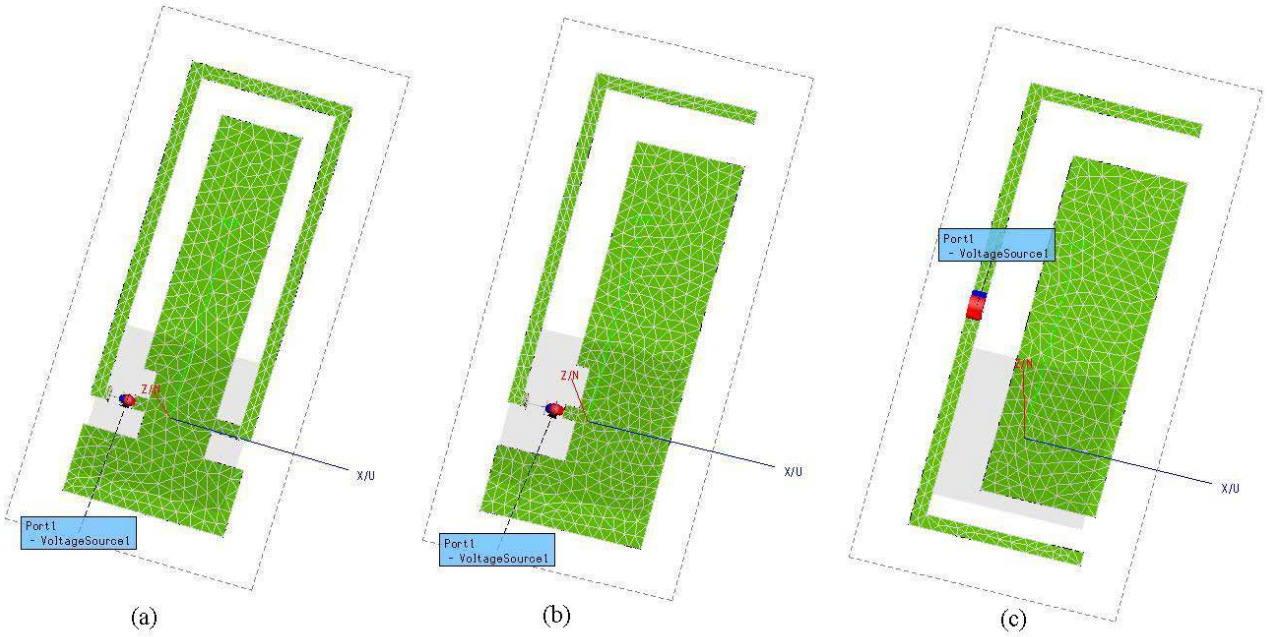

Fig. 1. Geometry of small antennas: a) loop antenna, b) whip antenna, and c) dipole antenna.

2) Case 2. Antenna electrically connected to a metal rim

In order to analyze these three types of antennas in their intended environment, a metal rim is imported into the model. In this case, as shown in Fig 2, the rim is placed 15 mm below the PCB, but electrically connected to the ground plane by a 2-mm wide conducting trace. The rim is modeled as a metal cylinder with a diameter of 430 mm and width of 225 mm. The PCB is placed 15 mm away from the width center of the cylinder which is closed to the actual location of the tire valve.

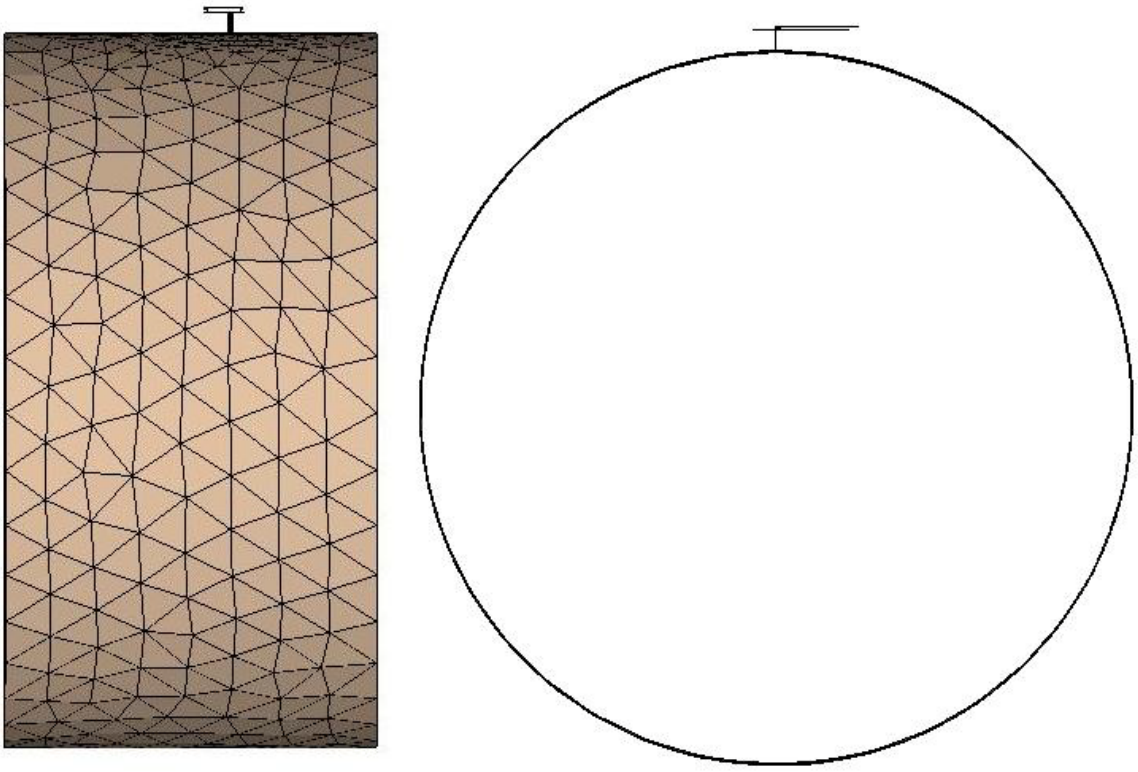

Fig. 2. Model for antenna with a metal cylinder electrically attached below.

3) Case 3: Antenna above rim with no electrical contact

Fig. 3 illustrates the antenna located above the rim without making electrical contact. The model parameters are as the same as the model in Case 2 except no conducting trace is placed between the metal cylinder and the PCB.

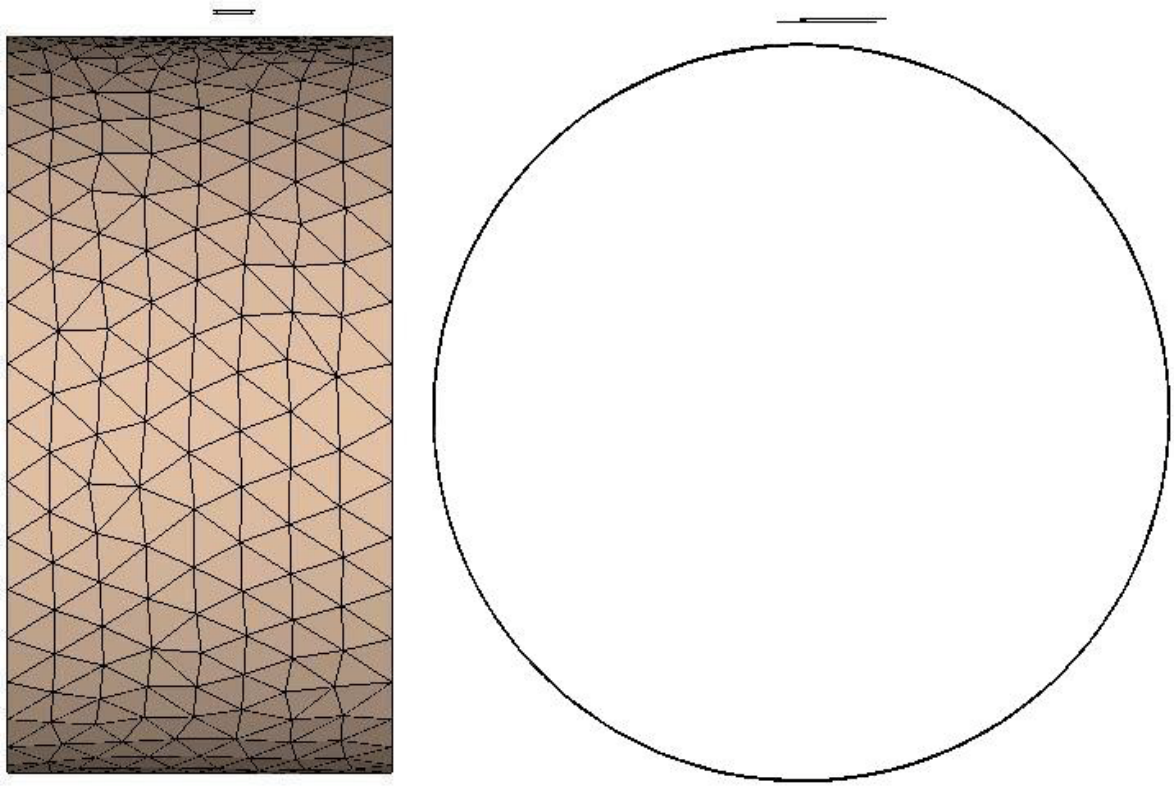

Fig. 3. Model for antenna above a metal cylinder.

4) Results for the three cases above

The input impedances and radiation efficiencies at 315 MHz for the loop antenna, whip antenna, and dipole antenna made from PCB traces in the three cases described above are calculated using full wave simulations [5]. The results are summarized in Table 1.

Table 1. Some results for the PCB trace antennas

Parameters		Loop Antenna	Whip Antenna	Dipole Antenna
Input Impedance (ohm)	Case 1	0.463+j222.0	0.499+j(-493.2)	0.170+j(-693.6)
	Case 2	0.513+j226.7	0.717+j(-376.6)	0.056+j(-691.5)
	Case 3	0.408+j214.8	0.280+j(-480.3)	0.056+j(-691.5)
Radiation Efficiency	Case 1	13.2%	50.3%	71.5%
	Case 2	15.5%	64.1%	14.0%
	Case 3	2.1%	11.4%	11.6%

For the antenna structures without the rim (Case 1), the loop antenna has the lowest efficiency; both the whip and dipole antennas have efficiencies greater than 50 percent. In Case 2, when the metal rim model is imported and electrically connected to the ground of the PCB, the efficiencies for both the loop and whip antenna are improved while the efficiency of the dipole antenna decreases. For Case 3, when the conducting rim is imported but not connected to the PCB ground, all efficiencies decrease. The loop antenna efficiency is only a few percent, while the other two have efficiencies barely above 10 percent.

C. Antenna Employing a Separate Raised Metal Piece

1) Antenna model in three cases

Antennas were also designed using a piece of metal that extended above the surface of the PCB. This kind of antenna is usually driven single-ended. The far end is either left open (whip type antenna) or shorted to the ground plane of the PCB (loop type antenna). Fig. 4 shows the geometry of these two antennas, which are both located 10 mm away from the edge of the PCB. The raised height is 5 mm and the length of the antenna along the short edge of the PCB is 20 mm. The board has the same dimensions as in Part B and the three simulation cases are also same as those in Part B.

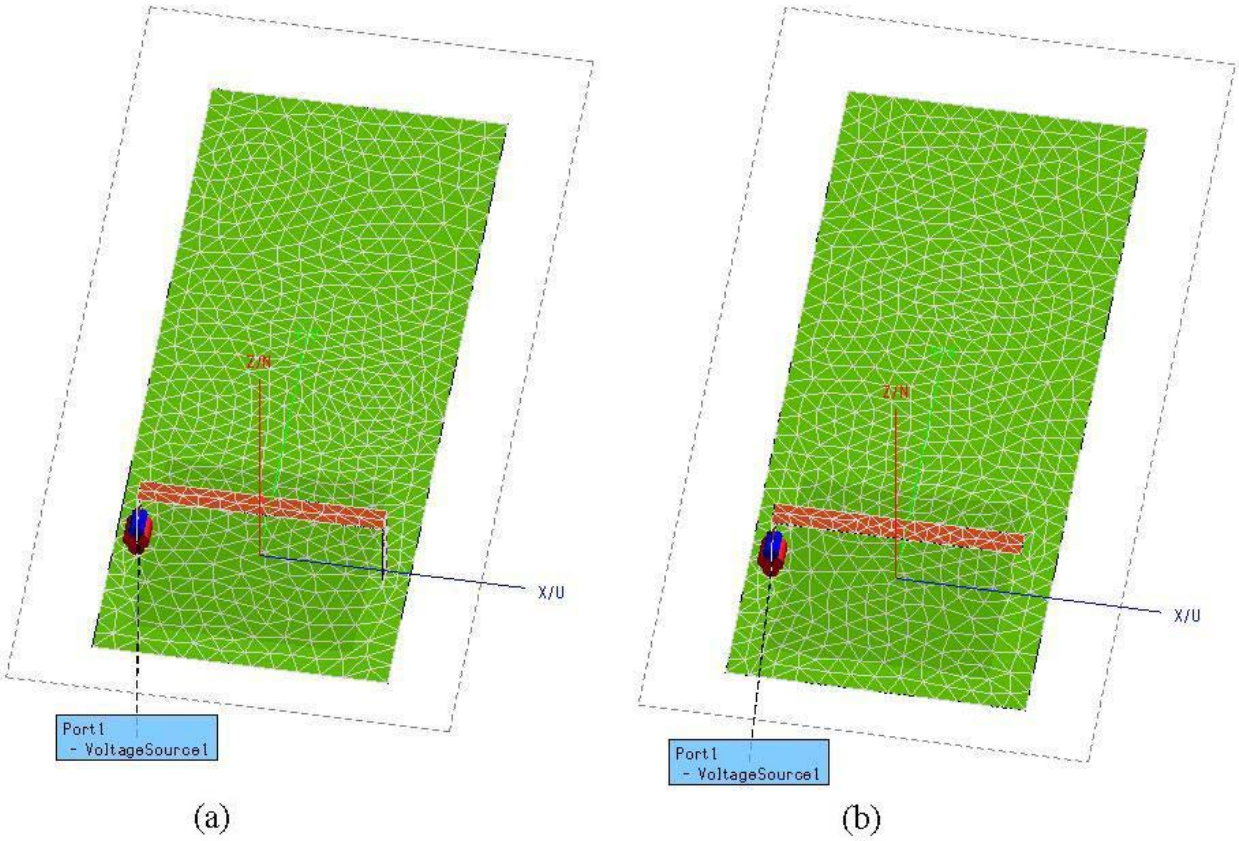

Fig. 4. Geometry of small raised-height antennas: a) loop antenna, b) whip antenna.

2) Results

Table 2 lists the input impedance and radiation efficiency at 315 MHz for these raised-height antennas. The input impedances for the loop antenna are more consistent in the three cases than those of the whip antenna. However, the radiation efficiencies for the whip antenna are more than 80 percent in all three cases; while the efficiency of the loop type antennas are only a few percent.

Table 2. Some results for the metal antennas.

Parameters		Loop Antenna	Whip Antenna
Input Impedance (ohm)	Case 1	0.0458+j40.1	0.0933+j(-1047.7)
	Case 2	0.0470+j40.1	0.3173+j(-1022.7)
	Case 3	0.0469+j40.1	0.0905+j(-1044.6)
Radiation Efficiency	Case 1	1.8%	86.5%
	Case 2	4.2%	95.3%
	Case 3	3.9%	86.0%

The near fields for these raised-height antennas in each of the three cases are calculated as shown in Fig. 5 to Fig.7 respectively. Although in some directions, the near electric fields of the whip antenna are more significant than those of the loop antenna, the near magnetic fields of the loop antenna are greater than those of the whip antenna in all selected directions.

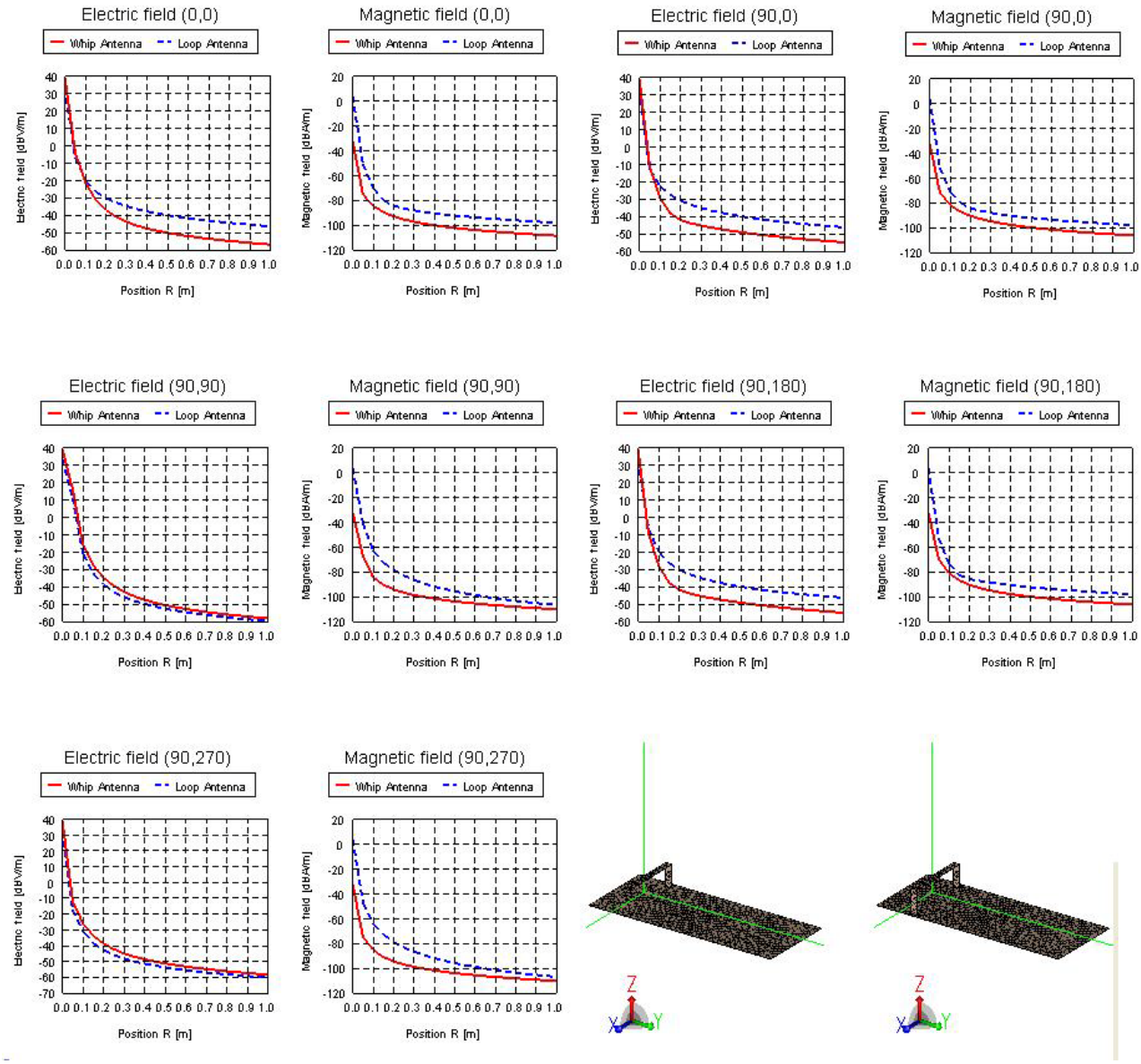

Fig. 5. Near fields in Case 1.

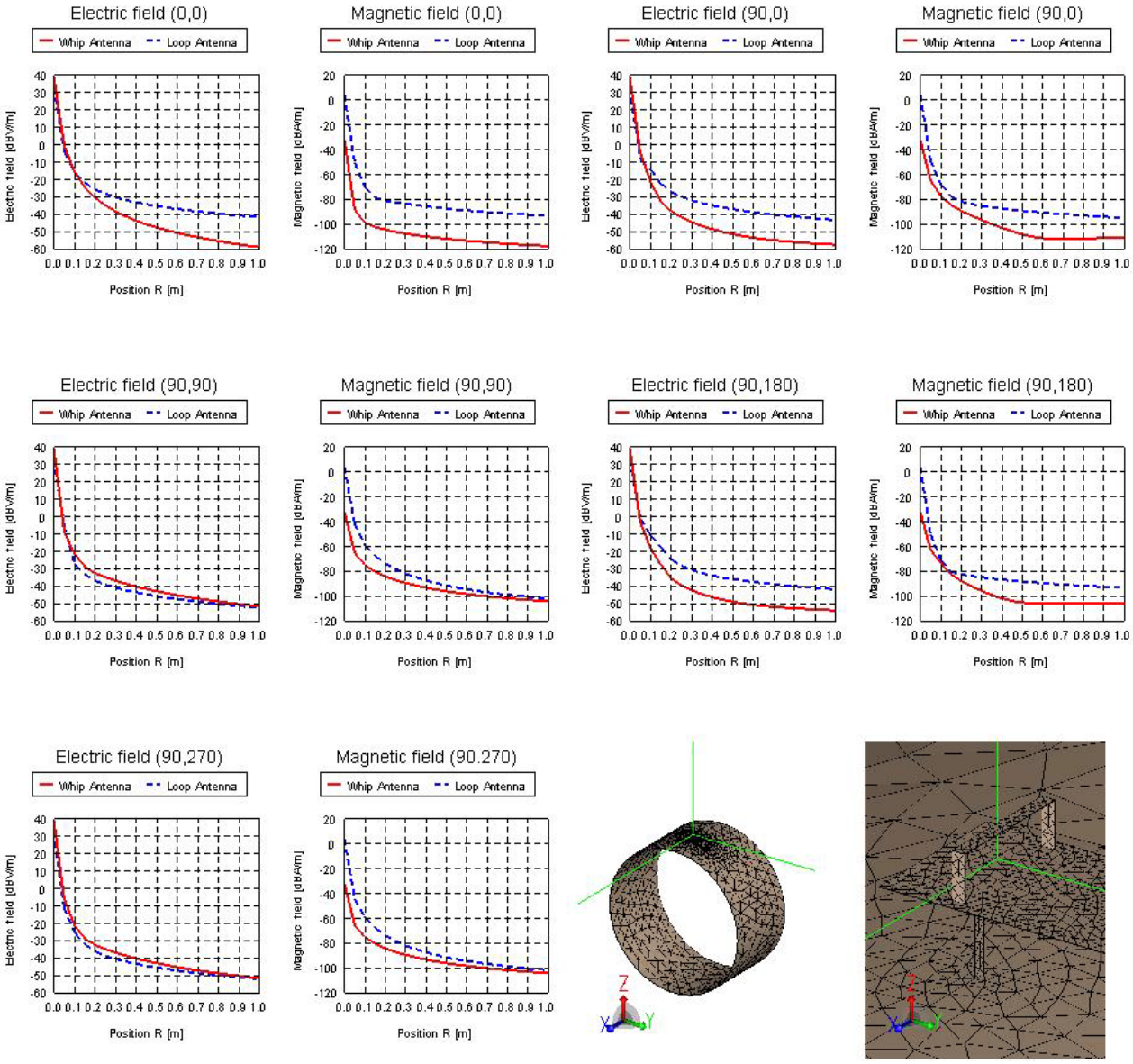

Fig. 6. Near fields in Case 2.

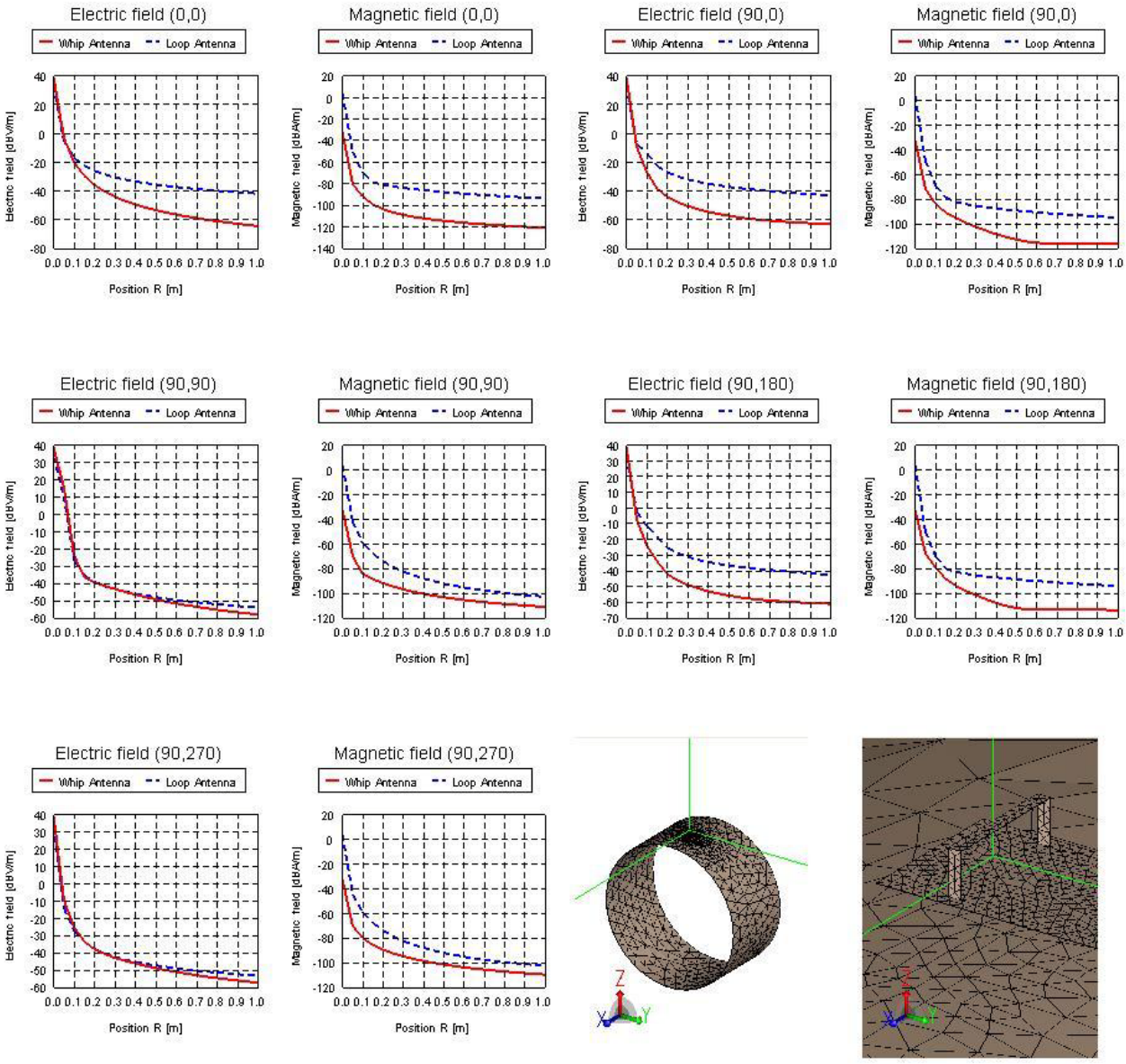

Fig. 7. Near fields in Case 3.

III. Matching Network

Note that the radiation resistance is extremely small, even for the whip antenna in some cases, which have efficiencies closed to 100 percent. Matching the antenna impedance to the transmitter output in order to minimize the mismatch losses is a significant challenge. Complexity is increased when the dissipative losses from all matching components are taken into account. In this report, a

process for designing a simple reactance-matching network is introduced. The derivation and applications details will not be discussed here.

A. Equivalence between series and parallel circuits.

Series and parallel circuits can be generally represented as indicated in Fig.8. The relationship of the resistance and reactance between these two circuits can be determined by equating their impedances.

$$R_s + jX_s = \frac{1}{\frac{1}{R_p} + \frac{1}{jX_p}} \tag{1}$$

By equating the real and imaginary parts, the resistance and reactance in one combination can be determined as a function of the other.

$$R_s = R_p\left(\frac{X_p^2}{R_p^2 + X_p^2}\right),\ X_s = X_p\left(\frac{R_p^2}{R_p^2 + X_p^2}\right) \text{ or} \tag{2}$$

$$R_p = \frac{R_s^2 + X_s^2}{R_s},\ X_p = \frac{R_s^2 + X_s^2}{X_s} \tag{3}$$

These can be expressed in terms of the quality factor Q as

$$R_s = R_p\left(\frac{1}{1+Q_p^2}\right),\ X_s = X_p\left(\frac{Q_p^2}{1+Q_p^2}\right) \text{ or} \tag{4}$$

$$R_p = R_s\left(1+Q_s^2\right),\ X_p = X_s\left(\frac{1+Q_s^2}{Q_s^2}\right) \tag{5}$$

where $Q_p = R_p/X_p$, $Q_s = X_s/R_s$. Q is defined as a ratio of stored to dissipated energy per cycle in a circuit.

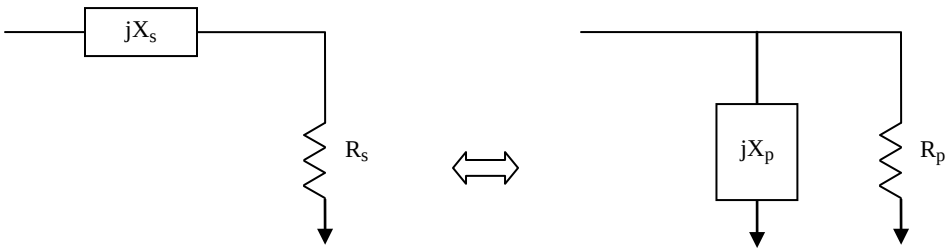

Fig. 8. Series and parallel representations of a circuit

B. Calculation of matching network

The simplest matching network is shown in Fig.9. It could be a split capacitor or split inductor matching network. The purpose of the matching network is to transform the antenna's small series resistance, R_A, to a desired larger value, R_{in}, to reduce the mismatch loss.

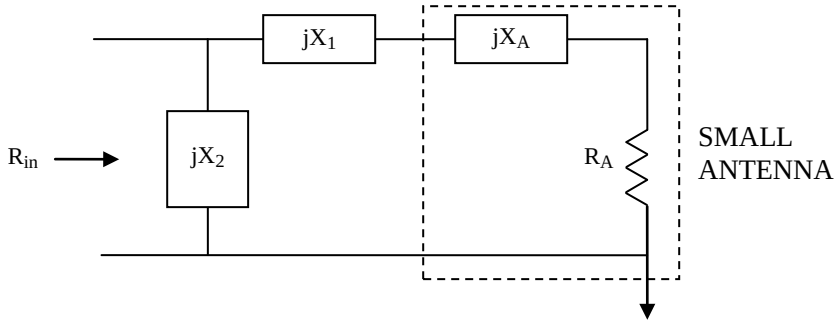

Fig. 9. Reactance matching network.

Let $R_s = R_a$, $R_p = R_{in}$, $X_s = X_a + X_1$, by applying (5) the following expressions can be obtained,

$$R_{in} = R_A\left(1+Q_s^2\right) \tag{6}$$

$$X_p = \left(X_A + X_1\right)\left(\frac{1+Q_s^2}{Q_s^2}\right) \tag{7}$$

$$Q_s = \frac{X_A + X_1}{R_A}. \tag{8}$$

Given the desired input resistance, R_{in}, X_1 can be determined from (8), X_2 is required to be equal in amplitude and opposite in sign to X_p to make the circuit resonant. Therefore,

$$X_1 = Q_s R_A - X_A \tag{9}$$

$$X_2 = -\left(X_A + X_1\right)\left(\frac{1+Q_s^2}{Q_s^2}\right) \tag{10}$$

where $Q_s = \sqrt{\frac{R_{in}}{R_A} - 1}$. (11)

In this application, a split capacitor matching network is used to match the small loop antenna, which can be represented as a series combination of a resistance R_A and inductance L_A. Solving (9) and (10) results in the solutions for C_1 and C_2,

$$C_1 \approx \frac{1}{4\pi^2 f^2 L_A - 2\pi f\sqrt{R_{in}R_A}} \tag{12}$$

$$C_2 \approx \frac{1}{2\pi f\sqrt{R_{in}R_A}}. \tag{13}$$

Typically C_2 will be much larger than C_1. In this case, C_1 tunes the resonant frequency while C_2 independently tunes the antenna impedance.

Similarly, a split inductor matching network is used to match the small whip and small dipole antenna, which can be represented as a series combination of a resistance R_A and capacitance C_A. The values of L_1 and L_2 can be solved in the same way as above,

$$L_1 \approx \frac{\sqrt{R_{in}R_A}}{2\pi f} + \frac{1}{4\pi^2 f^2 C_A} \tag{14}$$

$$L_2 \approx \frac{\sqrt{R_{in}R_A}}{2\pi f}. \tag{15}$$

V. CONCLUSIONS

Comparing the radiation efficiencies of the antennas evaluated above, the whip antenna employing the exterior raised metal piece has the best overall efficiency. Electrically connecting the antenna ground to the metal rim improves the radiation efficiency of this system. However, this does not mean the whip antenna is the best antenna for TPMS applications. The whip antenna has a smaller near magnetic field than the loop antenna. When the vehicle body is imported into the model, the coupling between the transmitter and receiver may be dominated by the near magnetic fields. Furthermore, due to the larger capacitive part of the input impedance for the whip antenna, the inductor matching network is more difficult to implement than it is for the capacitor matching network required for the loop antenna. The higher quality factor of the whip antenna results in a narrower bandwidth that can be more difficult to tune and control.

REFERENCES

[1] V. Kukshya, H.J. Song, H.P. Hsu, and R.W. Wiese, "Characterizing performance of tire pressure monitoring systems using experimental measurements and system simulations," *Proc. of IEEE International Symposium on Antennas and Propagation*, Honolulu, HI, USA, June 2007, pp. 4112-4115

[2] K. Tanoshita, K. Nakatani, and Y. Yamada, "Electric field simulations around a car of the tire pressure monitoring system," *IEICE Trans. on Communications,* vol. E90-B, no. 9, pp. 2416-2422, Sept. 2007.

[3] H.J. Song, H.P. Hsu, R. Wiese, and T. Talty, "Modeling signal strength range of TPMS in automobiles", *Proc of IEEE International Symposium on Antennas and Propagation*, Sendai, Japan, Aug. 2004, pp. 3167-3170.

[4] M. Brzeska, and G.-A. Chakam, "RF modeling and characterization of a tyre pressure monitoring system," *Proc of 2nd European Conference on Antennas and Propagation*, Edinburgh, UK, Nov. 2007, pp. 1-6.

[5] *FEKO User Manual, Suite 5.4*, 2008.